Effect of Confinement on High-Strength Concrete Circular Columns Reinforced with GFRP Bars and Spirals

Mu'taz Almomani and Ehab El-Salakawy

1 Introduction

Corrosion is a major drawback to the use of conventional steel reinforcement. Although it may be delayed, corrosion is a phenomenon related to the nature of steel and cannot be completely eliminated (ACI 222 2019; ACI 440 2015). The susceptibility to corrosion increases in North America due to common use of de-icing salts and extreme weather conditions. Fibre Reinforced Polymer (FRP) reinforcement has many advantages over steel. These include a higher tensile strength, lower density, electromagnetic transparency and non-corrodibility (ISIS Canada 2007). Many recent works have studied structural elements reinforced with FRP (Ghomi et al. 2015; Mahmoud et al. 2016; Hadhood et al. 2016). Results have confirmed the adequacy of FRP as the main concrete reinforcement. Circular columns have also been studied under different loading conditions (Ali et al. 2015; Kharal et al. 2016; Hadhood et al. 2017). Studies have shown FRP to resist axial and lateral loads similar to steel reinforced concrete (RC). The higher loads from high-rise buildings and bridges necessitate the use of higher capacity materials such as high-strength concrete (HSC). However, there still is a lack of data on FRP-reinforced High-Strength Concrete (FRP-RHSC) columns under eccentric loading. The aim of this study is to evaluate the performance of GFRP-RHSC circular columns under eccentric loads.

M. Almomani · E. El-Salakawy (✉)
Department of Civil Engineering, University of Manitoba, Winnipeg, MB, Canada
e-mail: Ehab.El-Salakawy@umanitoba.ca

M. Almomani
e-mail: Almomanm@myumanitoba.ca

B. Benmokrane et al. (eds.), *8th International Conference on Advanced Composite Materials in Bridges and Structures*, Lecture Notes in Civil Engineering 278,
https://doi.org/10.1007/978-3-031-09632-7_32

2 Experimental Program

2.1 Specimen Details

Three large-scale HSC circular columns were constructed and testing in this study. Two columns were reinforced with GFRP bars and spirals. The third one was reinforced with steel reinforcement. The specimens had a 350 mm diameter and were 1,750 mm in length. The Canadian standards and codes for steel and FRP were used to design the steel and GFRP columns, respectively. Six sand-coated GFRP No. 16 (15.9 mm diameter) were used as longitudinal reinforcement, and No. 10 (9.5 mm diameter) were used as GFRP spirals. For the steel specimen, six No. 15 M bars and a No. 10 M spiral were used. The reinforcement properties are summarised in Table 1.

The columns were cast with 60 MPa concrete and cover of 25 mm to the spirals was maintained. The spiral pitch of the steel control specimen was set at 85 mm and a pitch of 50 mm and 85 mm was used for the GFRP specimens. The specimen names are composed of two parts. The letter "G" or "S" indicates the type of reinforcement (GFRP or Steel). The second part indicated the spiral pitches "85" or "50". The test matrix is summarised in Table 2. The concrete strength, provided in Table 1, was obtained on the day of testing the column.

Table 1 Reinforcement properties

Bar No	Bar diameter (mm)	Area of bar (mm^2)	Modulus of elasticity (GPa)	Tensile strength (MPa)
Steel				
No. 10 M	11.3	100	200	470
No. 15 M	16.0	200	200	480
GFRP				
No. 10	9.5	71	50	1,022
No. 16	15.9	199	62	1,184

Table 2 Test matrix

<table>
<tr><th rowspan="2">Specimen ID</th><th>Longitudinal reinforcement</th><th colspan="2">Transverse reinforcement</th><th rowspan="2">Concrete strength (MPa)</th></tr>
<tr><th>Reinforcement ratio (%)</th><th>Spiral pitch (mm)</th><th>Reinforcement ratio (%)</th></tr>
<tr><td>S-85</td><td rowspan="3">1.24</td><td>85</td><td>1.78</td><td>58.8</td></tr>
<tr><td>G-50</td><td>50</td><td>1.89</td><td>59.4</td></tr>
<tr><td>G-85</td><td>85</td><td>1.26</td><td>60.3</td></tr>
</table>

Fig. 1 Test setup

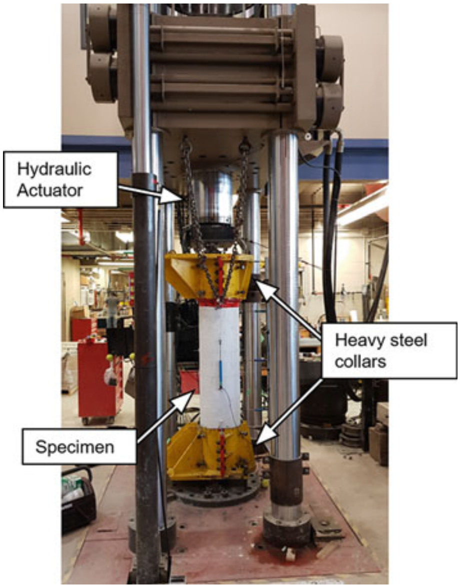

2.2 *Instrumentation and Test Setup*

A combination of LVDTs, strain gauges and PI-gauges were used to monitor the behavior of the column. LVDTs were used to measure the lateral deflection of the column as well as the axial displacement. Strain gauges were attached to reinforcement at critical locations to monitor the strains in the bars in addition to a concrete strain gauge to measure the strain in the outermost compression zone. PI-gauges were also placed at the maximum compression and tension zone of the columns to measure strains.

The column was tested under axial loading at 60 mm eccentricity. This was achieved by using specially constructed steel collars with a pin welded at the required eccentricity from the centre to provide pin-pin boundary conditions. The load was applied using a 5000-kN capacity hydraulic actuator. The loading was displacement-controlled at a rate of 1.5 mm/min. Figure 1 highlights the main components of the test setup.

3 Results and Discussion

3.1 *Column Displacement Response*

The column vertical (axial) displacement and the mid-height lateral displacement increased gradually for all columns until the peak load. The data was recorded for

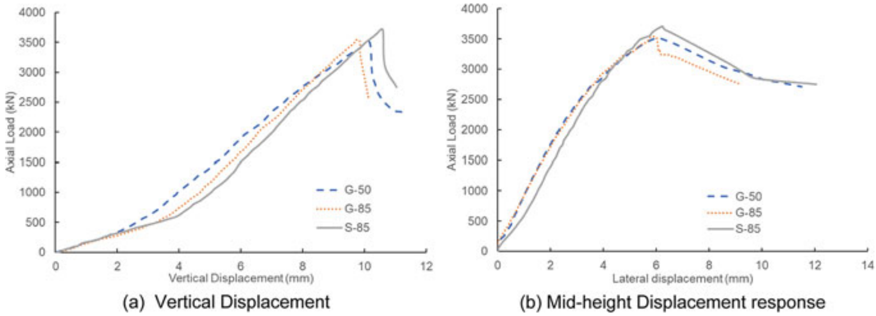

Fig. 2 Load versus vertical and lateral displacement

each column until the axial load dropped by 25% from the peak load. The maximum vertical displacements measured were 10.1 mm, 11.0 mm and 11.3 mm for specimens G-85, G-50 and S-85, respectively. The vertical displacement response is shown in Fig. 2a.

The maximum lateral displacements recorded were 9.2 mm, 11.5 mm and 12.1 mm for specimens G-85, G-50 and S-85, respectively. At the peak load, the displacement continued to increase as the load carried by the column decreased sharply. Similar patterns can be seen in Fig. 2b. The columns mid-height section deflected from the vertical axis gradually as the column was loaded and after the load reached the peak, the load started to decrease while the deflection increased further. Additionally, lateral deflection showed gradual increase of displacement over the post-peak portion of the curves. The responses recorded for G-50 and G-85, reinforced with GFRP, were very similar to the control specimen S-85, reinforced with steel reinforcement. The vertical and lateral deflections were both relatively small and this was due to the high stiffness of the HSC.

3.2 Load Capacity and Mode of Failure

The maximum load capacities were 3,540, 3,511 and 3,708 kN for columns G-85, G-50 and S-85, respectively. No tension cracks were visible until the peak load of each column was reached. The columns failed due to crushing of concrete. No signs of spalling were visible before this point. The test was stopped after the loss of 25% of the peak axial load. After the spalled concrete was removed, vertical cracks were seen in the concrete core of all three columns. No bar or spiral ruptures were observed and the failure for the GFRP-RC specimen was similar to the steel specimen and no violent rupture of GFRP bars was observed (Fig. 3).

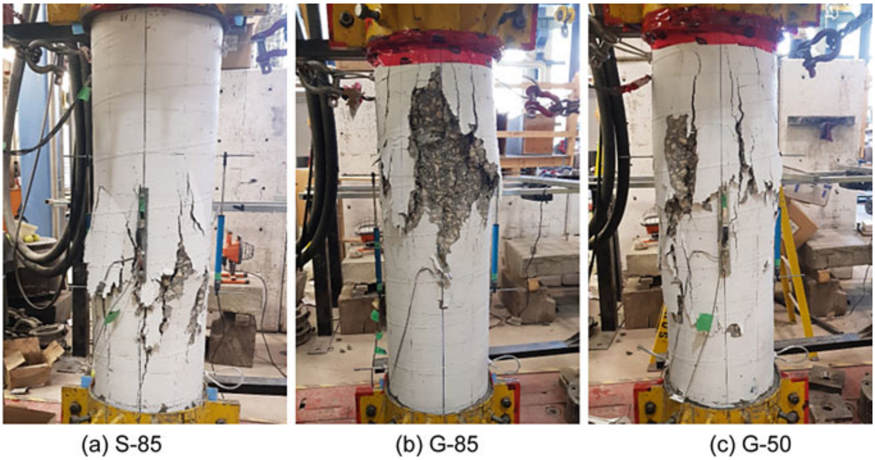

Fig. 3 Specimen Failure modes

4 Conclusions

The experimental results of three large-scale HSC circular columns tested under eccentric loads have been presented in this paper. Based on the observations made, the main findings are as follows:

1. Both GFRP-RHSC columns were able to achieve approximately 95% of the peak load of the steel reinforced counterpart.
2. The increase in the pitch of the GFRP spirals from 85 mm to 50 mm increased the lateral displacement by approximately 21%. However, it had no significant effect on the axial capacity of columns.
3. The mode of failure of the GFRP-RC columns was very similar to that of their steel counterpart. All failed with spalling of the concrete cover followed by crushing of the concrete core.
4. Although the maximum lateral displacements were very small, displacement of the GFRP-RC column with a spiral pitch of 85 mm was 24% less than that of the steel counterpart with the same pitch.

Acknowledgements The Authors would like to express their thanks to the Natural Science and Engineering Research Council of Canada (NSERC) for their financial support and to the technical staff at the W.R. McQuade Heavy Structures Laboratory at the University of Manitoba for their assistance.

References

ACI COMMITTEE 222 (2019) Guide to protection of metals in concrete against corrosion, ACI 222R-19. American Concrete Institute (ACI), Farmington Hills, Detroit, MI

ACI COMMITTEE 440 (2015) Guide for the Design and Construction of Structural Concrete Reinforced with Fiber-Reinforced Polymer (FRP) Bars, ACI 440.1R-15. Americal Concrete Institute (ACI), Farmington Hills, Detroit, MI

Ali MA, El-Salakawy E (2015) Seismic performance of GFRP-reinforced concrete rectangular columns. J. Compos. Constr. 20(3):04015074

ISIS CANADA (2007) Reinforcing concrete structures with fibre reinforced polymers, Design Manual No.3. ISIS Canada corporation, University of Manitoba, Winnipeg, Canada, p 103

Ghomi SK, El-Salakawy E (2015) Seismic performance of GFRP-RC exterior beam–column joints with lateral beams. J. Compos. Constr. 20(1):04015019

Hadhood A, Mohamed HM, Benmokrane B (2016) Axial load–moment interaction diagram of circular concrete columns reinforced with CFRP bars and spirals: experimental and theoretical investigations. J. Compos. Constr. 21(2):04016092

Hadhood A, Mohamed HM, Benmokrane B (2017) Strength of circular HSC columns reinforced internally with carbon-fiber-reinforced polymer bars under axial and eccentric loads. Constr. Build. Mater. 141:366–378

Kharal Z, Sheikh SA (2016) Behaviour of concrete columns with GFRP circular and rectilinear confining reinforcement. Resilitent Infrastruct. 1–11

Mahmoud K, El-Salakawy E (2016) Size effect on shear strength of glass fiber-reinforced polymer-reinforced concrete continuous beams. ACI Struct. J. 113(1):125–134